Nanocrystal targeting *in vivo*

Maria E. Åkerman*†‡, Warren C. W. Chan†‡, Pirjo Laakkonen*, Sangeeta N. Bhatia†, and Erkki Ruoslahti*§

*Cancer Research Center, The Burnham Institute, 10901 North Torrey Pines Road, La Jolla, CA 92037; and †Department of Bioengineering, University of California at San Diego, 9500 Gilman Drive, La Jolla, CA 92093

Contributed by Erkki Ruoslahti, August 1, 2002

Inorganic nanostructures that interface with biological systems have recently attracted widespread interest in biology and medicine. Nanoparticles are thought to have potential as novel intravascular probes for both diagnostic (e.g., imaging) and therapeutic purposes (e.g., drug delivery). Critical issues for successful nanoparticle delivery include the ability to target specific tissues and cell types and escape from the biological particulate filter known as the reticuloendothelial system. We set out to explore the feasibility of *in vivo* targeting by using semiconductor quantum dots (qdots). Qdots are small (<10 nm) inorganic nanocrystals that possess unique luminescent properties; their fluorescence emission is stable and tuned by varying the particle size or composition. We show that ZnS-capped CdSe qdots coated with a lung-targeting peptide accumulate in the lungs of mice after i.v. injection, whereas two other peptides specifically direct qdots to blood vessels or lymphatic vessels in tumors. We also show that adding polyethylene glycol to the qdot coating prevents nonselective accumulation of qdots in reticuloendothelial tissues. These results encourage the construction of more complex nanostructures with capabilities such as disease sensing and drug delivery.

Hybrid organic/inorganic nanoparticles are thought to have potential as novel intravascular probes for diagnostics (e.g., imaging) and therapeutics (e.g., drug delivery) (1). For this potential to be realized, an ability to target the nanoparticles to specific tissues and cell types would be important. We used semiconductor quantum dots (qdots) coated with targeting peptides as prototypic nanostructures for intravascular delivery in live mice. Qdots are generally composed of atoms from groups II–VI or III–V of the periodic table and are defined as particles with physical dimensions smaller than the exciton Bohr radius (2). This size leads to a quantum confinement effect, which endows nanocrystals with unique optical and electronic properties. Qdots have size-tunable emission (from the UV to the IR), narrow spectral line widths, high luminescence, continuous absorption profiles, and stability against photobleaching (2–4). Furthermore, the large surface area-to-volume ratio of qdots makes them appealing for the design of more complex nanosystems.

Blood vessels express molecular markers that distinguish the vasculature of individual organs, tissues, and tumors. Peptides that recognize these vascular markers have been identified by screening phage libraries *in vivo*, a procedure in which peptides direct phage homing to individual sites (5). This approach has led to the identification of a unique set of homing peptides with high *in vivo* selectivity (6–9). We have used homing peptides to target i.v.-injected qdots to specific vascular sites in mice (Fig. 1). One of these peptides binds to membrane dipeptidase on the endothelial cells in lung blood vessels (9), and the other two preferentially bind to tumor blood vessels (10) or tumor lymphatic vessels (11) and the tumor cells. Each of the peptides directed the qdots to the appropriate site in the mice, showing that nanocrystals can be targeted *in vivo* with an exquisite specificity.

Materials and Methods

Preparation of Qdots and Peptide-Coated Qdots. Previously published procedures were used to synthesize tri-*n*-octylphosphine oxide-coated ZnS-capped CdSe qdots (12–15) and to modify their surface chemistry to render them water soluble (16, 17). After this step, the surface of qdots was coated with mercaptoacetic acid.

Three peptides were used to coat qdots: CGFECVRQCPERC peptide (denoted as GFE) binds to membrane dipeptidase on the endothelial cells in lung blood vessels (9, 18), KDEPQRRSARLSAKPAPPKPEPKPKKAPAKK (F3) preferentially binds to blood vessels and tumor cells in various tumors (10), and CGNKRTRGC (LyP-1) recognizes lymphatic vessels and tumor cells in certain tumors (11). The peptides were synthesized by *N*-(9-fluorenylmethoxycarbonyl)-L-amino acids chemistry with a solid-phase synthesizer and purified by HPLC. The composition of the peptides was confirmed by MS.

The peptides were thiolated by using 3-mercaptopropionimidate hydrochloride (a.k.a. iminothiolane), an imidoester compound containing a sulfhydryl group. Peptides were incubated with iminothiolane for 1 h in 10 mM PBS, pH 7.4, at a 1:1 molar ratio. Afterward, mercaptoacetic acid-coated qdots were added to the solution to exchange some of the mercaptoacetic acid groups with the thiolated peptide incubated overnight at room temperature. For coadsorption of polyethylene glycol (PEG) and peptides, amine-terminated PEG (Shearwater Polymers, Huntsville, AL) was thiolated with iminothiolane. Thiolated PEG was directly added to a solution of mercaptoacetic acid-coated qdots in 10 mM PBS, pH 7.4, and allowed to incubate overnight at room temperature. Afterward, the thiolated peptide was added to the PEG/qdot solution and incubated overnight at room temperature. The coated qdots were purified with Microspin G-50 columns (Amersham Pharmacia) before assays or injection into a mouse. The coupling efficiency was determined by performing a Bradford assay (Bio-Rad) on the coated qdots.

Mice, Cell Lines, and Tumors. Lung endothelial (LE), brain endothelial, and human breast carcinoma MDA-MD-435 cells were maintained as described (7, 18). To establish tumor xenografts, 10^6 exponentially growing MDA-MB-435 tumor cells were injected s.c. in the chest area of BALB/c *nu/nu* mice (Animal Technologies, Livermore, CA). The mice were used for *in vivo* targeting experiments 8–12 weeks after the tumor cell inoculation.

Qdot Injections and Histology. Peptide-coated qdots (100–200 μg in 0.1–0.2 ml PBS) were injected into the tail vein of a mouse and allowed to circulate for 5 min (GFE qdots) or 20 min (F3 and LyP-1 qdots). Blood vessels were visualized by i.v. injecting tomato lectin conjugated with either fluorescein or biotin (Vector Laboratories), as reported (11). While still under anesthesia, the mouse was perfused with 4% paraformaldehyde through the heart. Tissues were frozen in Tissue Tek OCT embedding medium (Sakura Finetek, Torrance, CA) before sectioning. The sections were mounted with Vectashield mounting medium with or without 4′,6-diamidino-2-phenylindole, dihydrochloride (Vector Laboratories) to visualize cell nuclei before examination under an inverted fluorescent microscope or a confocal microscope.

Abbreviations: qdot, quantum dot; PEG, polyethylene glycol; LE, lung endothelial.

‡M.E.Å. and W.C.W.C. contributed equally to this work.

§To whom correspondence should be addressed. E-mail: ruoslahti@burnham.org.

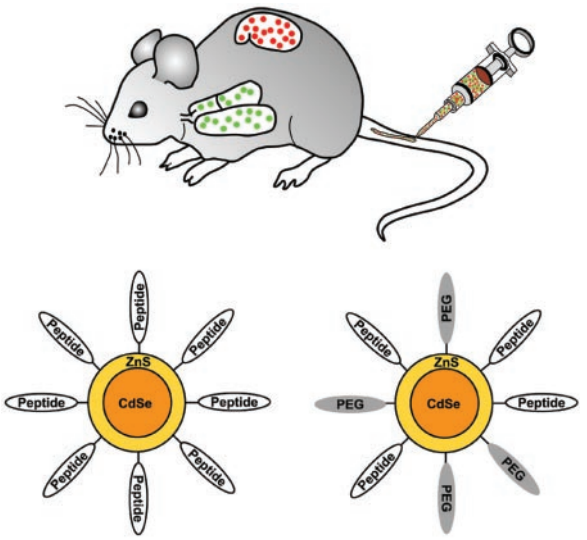

Fig. 1. Schematic representation of qdot targeting. Intravenous delivery of qdots into specific tissues of the mouse. (*Upper*) Design of peptide-coated qdots. (*Lower*) Qdots were coated with either peptides only or with peptides and PEG. PEG helps the qdots maintain solubility in aqueous solvents and minimize nonspecific binding.

Results

Peptide-Coated Qdots. We synthesized ZnS-capped CdSe qdots emitting in the green and the red (550 nm and 625 nm fluorescence maxima, respectively) and coated them with peptides by using a thiol-exchange reaction. The coupling of the GFE peptides yielded monodisperse qdots, whereas qdots coated with the F3 aggregated. The large number of positive residues in F3 may have caused colloidal aggregation by "bridging" negatively charged qdots. We overcame the aggregation problem by either decreasing the population of peptides on the qdot surface or by co-coupling peptides and PEG (molecular weight = 5,000 g/mol), a polymer known to minimize molecular interactions and improve colloidal solubilities (19) (Fig. 1). Protein assays revealed about 120 peptide molecules per qdot when peptide only was coupled. Co-coupling of PEG reduced this number to about 70.

Peptide Specificity *in Vitro*. To explore the binding activity and specificity of peptide-coated qdots, experiments were first conducted *in vitro*. LE and brain endothelial cells were grown in culture, and green-luminescent GFE-coated qdots were incubated with each cell type. The LE cells express membrane dipeptidase, the receptor for the GFE peptide, whereas the brain endothelial cells do not (9). On optical excitation, qdots coated with the lung-homing GFE peptide were observed decorating the surface of LE cells (Fig. 2*a*), whereas no visible signal was observed on the brain endothelial cells. Specificity of the GFE-qdot binding to LE cells was further demonstrated by inhibition of binding by both the addition of free GFE peptide or the organic molecule cilastatin, a known ligand and inhibitor of membrane dipeptidase (20) (Fig. 2 *b* and *c*). This finding was quantified by using digital image analysis (Fig. 2*d*).

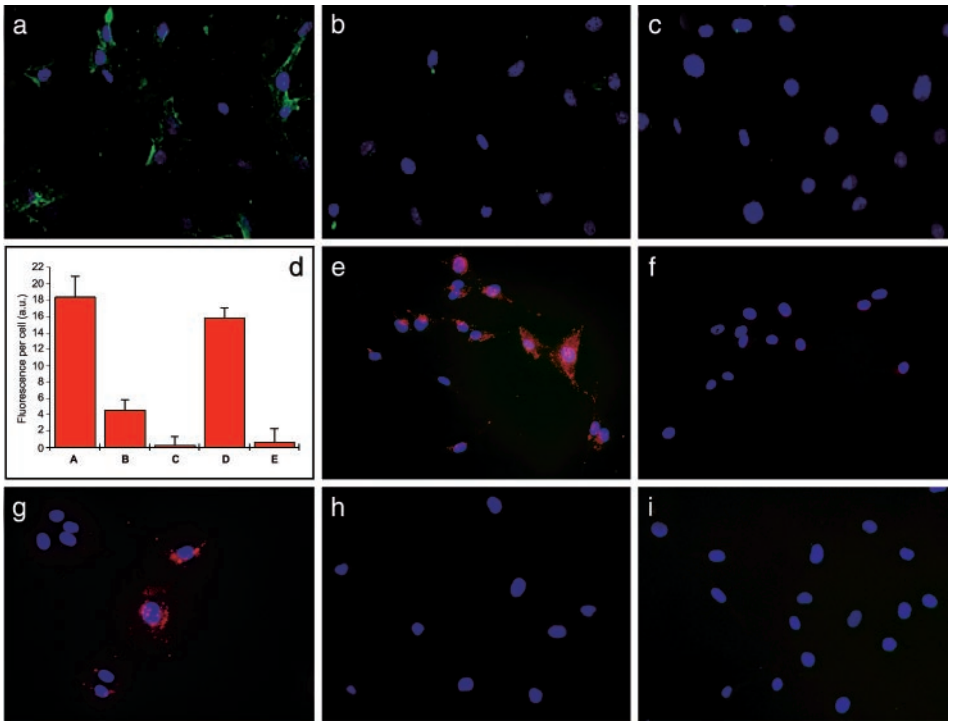

Fig. 2. Binding of peptide-conjugated qdots to endothelial cells and breast cancer cells *in vitro* is specific to peptide sequence. (*a*) Binding of green GFE-conjugated qdots to LE cells that express membrane dipeptidase. (*b* and *c*) Inhibition of GFE-qdot binding to LE cells by free GFE peptide (500 μM) (*b*) or with cilastatin, an inhibitor of the receptor, membrane dipeptidase (50 μM) (*c*). (*d*) Quantification of fluorescence intensity of an experiment similar to the one illustrated in *a*–*c*. (Columns A–C) GFE-qdot binding to LE cells; GFE concentration 250 μM; and cilastatin 50 μM. (Column D) The binding of GFE-qdots to the LE cells is not inhibited by a control peptide (LyP-1; 250 μM). (Column E) LyP-1-qdots do not bind to the LE cells. The fluorescence associated with 10 individual cells from each panel was measured by using digital image analysis. Background fluorescence from cells that received no qdots has been subtracted (2 a.u., arbitrary units). A representative experiment of five experiments was quantified. (*e* and *f*) F3 qdots bind to MDA-MB-435 breast carcinoma cells (*e*); free F3 peptide (500 μM) inhibits the binding (*f*). (*g*) Binding of LyP-1 qdots to MDA-MB-435 cells. (*h* and *i*) GFE qdots do not recognize the MDA-MB-435 cells (*h*) and LyP-1 qdots do not bind to the LE cells (*i*). Nuclei were visualized with 4′,6-diamidino-2-phenylindole staining (blue). Cells were examined under an epifluorescence microscope with a 425/40-nm excitation and a 515-nm long-pass filter. (Original magnifications: *a*–*c* and *i*, ×200; and *e*–*h*, ×400.)

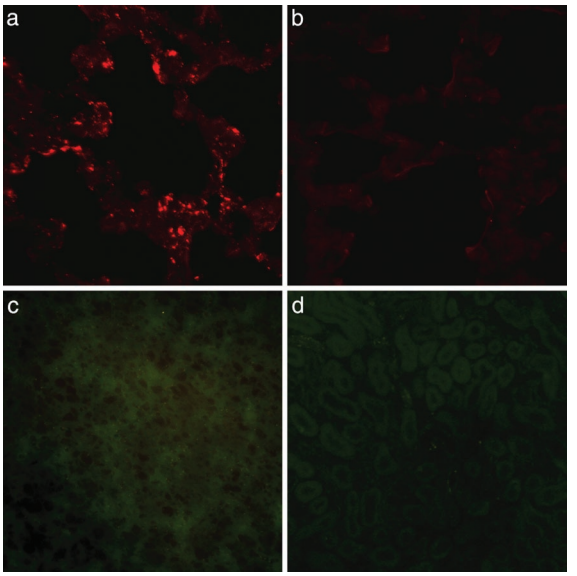

Fig. 3. *In vivo* targeting of qdots to normal lung vasculature is specific. Red GFE-conjugated qdots were injected into the tail vein of normal mice, and the presence of qdots in lung tissue was assessed by examining sections under a confocal microscope with UV excitation and a 585-nm long-pass filter (*a* and *b*) or an epifluorescent microscope as in Fig. 2 (*c* and *d*). (*a*) Red qdots localized in lung tissue. (*b*) Inhibition of qdot accumulation in the lungs by coinjected cilastatin. (*c* and *d*) Absence of GFE qdots in the brain (*c*) and kidney (*d*) demonstrates the specificity of binding. The results shown are representative of three experiments carried out with nine mice. (Original magnifications: *a* and *b*, ×600; *c* and *d*, ×200.)

Qdots coated with F3 or LyP-1 bound to the MDA-MB-435 human breast carcinoma cells (Fig. 2 *e* and *g*). As with GFE, specificity of F3- and LyP-1-coated qdots was demonstrated by inhibition of binding by the appropriate cognate peptide (shown for the F3 qdots in Fig. 2*f*), and further confirmed by lack of inhibition by an unrelated (GFE) peptide or by cilastatin (not shown). The GFE-coated qdots did not bind to the MDA-MB-435 cells (Fig. 2*h*), and LyP-1-coated qdots did not bind to the endothelial cells (Fig. 2*i*). These experiments show that coating with GFE, F3, or LyP-1 peptides endows qdots with specific affinity to their corresponding cellular target *in vitro*.

Qdot Homing to Lung Endothelium *in Vivo*. Next, the ability of peptide-coated qdots to home to their targets *in vivo* was examined. Because red luminescent qdots were easier to distinguish from the autofluorescent tissue background than the green luminescent qdots, we i.v. injected red qdots coated with GFE into normal BALB/c mice and studied the tissue distribution of the injected qdots 5 min later. We detected bright GFE-qdot luminescence in the lungs (Fig. 3*a*), and its appearance was inhibited when the qdots were coinjected with cilastatin, similar to the *in vitro* studies (Fig. 3*b*). The GFE qdots were not found in various other organs (Fig. 3*c*, brain and Fig. 3*d*, kidney), except those with a prominent reticuloendothelial component (see below). Furthermore, we did not observe any acute toxicity, even after 24 h of circulation, caused by the i.v. administration of these nanoparticles (i.e., overt thrombosis or signs of complement activation).

Qdot Homing to Tumor Vasculature *in Vivo*. Qdots coated with peptides that home to tumor vasculature were examined in an MDA-MB-435 xenograft tumor system. Intravenously injected F3-coated and LyP-1-coated qdots accumulated in these tumors. As expected from their specificity for tumor blood vessels (10) and lymphatic vessels (11), the F3 and LyP-1 qdots targeted distinct structures within the tumors. The signal from F3-coated qdots colocalized with coinjected blood vessel marker lectin (Fig. 4*a*). The LyP-1-coated qdots did not

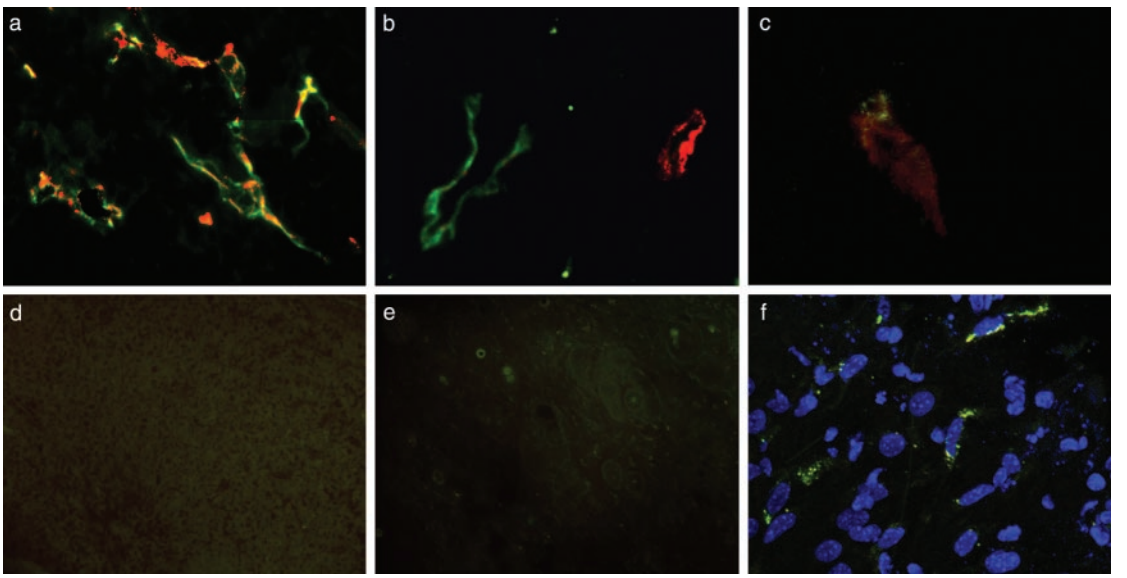

Fig. 4. *In vivo* targeting of qdots to tumor vasculature is specific. Red F3 or LyP-1 qdots, both PEG-coated, were injected into the tail vein of nude BALB/c mice bearing MDA-MB-435 breast carcinoma xenograft tumors. Blood vessels were visualized by coinjecting tomato lectin (green). (*a*) F3 qdots colocalize with blood vessels in tumor tissue. (*b*) LyP-1 qdots also accumulate in tumor tissue, but do not colocalize with the blood vessel marker. (*c*) Red F3 qdots and green LyP-1 qdots injected into the same tumor mouse target different structures in tumor tissue. (*d*) GFE qdots that bind to normal LE injected into tumor mice are not detected in tumor tissue. (*e*) F3 qdots injected into tumor mice do not appear in the skin taken from an area next to the tumor. A longer exposure was used in *d* and *e* to bring out the tissue background. (*f*) LyP-1 qdots are internalized by cells in tumor tissue. Images *a*, *b*, and *f* were obtained with a confocal microscope, and images *c*–*e* were obtained with an epifluorescent microscope as in Fig. 2. The results shown are representative of experiments carried out with six mice for the F3 qdots and 12 mice for the LyP-1 qdots. (Original magnifications: *a* and *d*, ×400; *b* and *c*, ×600; *e*, ×200; and *f*, ×2,400.)

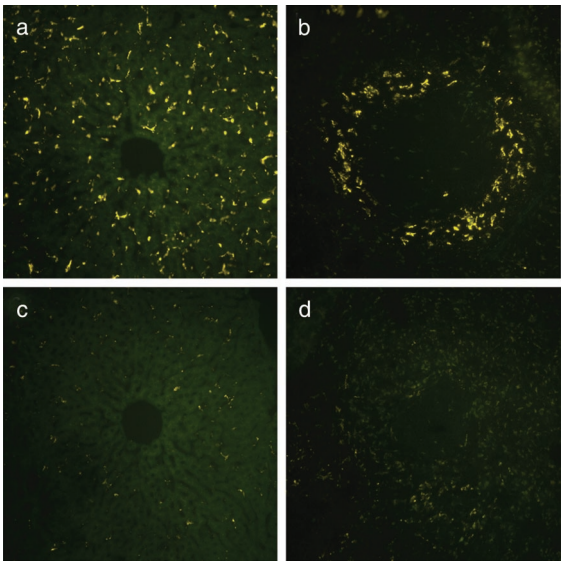

Fig. 5. Qdot uptake by the reticuloendothelial system is reduced by PEG coating. Green LyP-1 qdots with or without an added PEG coating were adjusted to an equal concentration by measuring absorbance at 540 nm and injected into the tail vein of mice bearing MDA-MB-435 tumors. Qdot localization in reticuloendothelial tissues was studied by epifluorescent microscopy of tissue sections as in Fig. 2. (*a* and *b*) LyP-1 qdots in the liver (*a*) and spleen (*b*). (*c* and *d*) LyP-1/PEG qdots in the liver (*c*) and spleen (*d*). These images are representative of three independent experiments. (Original magnifications: ×200.)

colocalize with the lectin (Fig. 4*b*) or F3 qdots (Fig. 4*c*). They did colocalize with the lymphatic vessel marker, podoplanin (21) (not shown), as has been shown previously for fluorescein-labeled LyP-1 peptide (11). GFE-coated qdots injected as a control were not detected in the tumors (Fig. 4*d*). Brain, heart, kidney, or skin did not contain detectable qdots (Fig. 4*e* and data not shown), indicating specificity of the F3 and LyP-1 qdots for tumor components. The regional specificity of qdot delivery within a tumor demonstrates the feasibility of targeting functionally distinct components of a tumor (e.g., blood vessels vs. lymphatics, etc.). Furthermore, the subcellular pattern of qdot luminescence suggests that peptide-coated nanostructures are internalized after binding to the cell surface, which may have implications for drug delivery and other applications that require intracellular targeting (Fig. 4*f*).

Elimination of the Nonspecific Uptake by the Reticuloendothelial System. The *in vivo*-injected qdots, regardless of the peptide used for the coating, accumulated in both the liver and spleen, in addition to the targeted tissues. The mononuclear phagocytes of the reticuloendothelial system, characterized by their ability to mediate nonspecific uptake of circulating particulates, apparently participated in the clearance of a fraction of circulating qdots in our experimental system. Adsorption-resistant coatings such as PEG are often used to minimize recognition by the reticuloendothelial system, thereby increasing circulation half-life (22). We prepared LyP-1 qdots with and without PEG coating and found that PEG nearly eliminated the nonspecific uptake into the liver and spleen (Fig. 5). Based on quantification of qdot fluorescence with digital image analysis, we estimate that coadsorption of PEG with peptide on the surface of qdots reduced the accumulation in the liver and spleen by about 95%. The PEG coating did not noticeably alter qdot accumulation in tumor tissue.

Discussion

In this article, we demonstrate the selective targeting of peptide-coated qdots to the vasculature of normal lungs and tumors, showing that it is possible to target hybrid organic/inorganic nanometer-sized colloidal material in a living mammal. In the future, the components and functions of a nanosystem will not be limited to peptide/semiconductor composites and luminescence.

Our peptide-coated qdots showed excellent homing specificity for the relevant vascular site, but we did not see accumulation of fluorescence within the targeted tissue. This finding is in contrast to what we have seen when the two tumor-homing peptides, F3 and LyP-1, were coupled to fluorescein. In that case, there was accumulation of fluorescence not only in the blood or lymphatic vessels, but also in the tumor cells. It is also possible that qdots did not penetrate into the tissue. The uncoated qdots have a diameter of 3.5 nm (green) or 5.5 nm (red) (14), which is equivalent to about 40 kDa, and the peptide coating adds another about 150 kDa. This may be a sufficiently large size to impede tissue penetration. However, F3 and LyP-1 qdots accumulated less well in cultured cells than the fluorescein-labeled peptide. It may be that the qdots were not sufficiently stable to remain luminescent in living cells and tissues. Alternatively, the fluorescence may be quenched by the qdots subjected to low pH in the microenvironment, by oxidation of the surface, or by factors adsorbed to the surface. For the delivery of nanocrystalline drugs, crystals that are unstable in tissue may offer an advantage, as the drug would dissolve at the target.

Our results suggest the potential selective targeting of other nanomaterials [e.g., optically active metallic colloids (23), near-IR emitting nanocrystals (24–26), and magnetic nanoparticles (27, 28)] as *in vivo* optical and magnetic probes for noninvasive imaging. The use of peptides to target drug-carrying nanostructures [such as those composed of fullerenes (29, 30) or dendrimers (31, 32), or stabilized drug nanocrystals] should also be possible. This targeting approach has been used recently to deliver nano-sized particles composed of lipids and DNA to tumor vasculature (33). Although the current nanosystems are rather simple, in the future we envision the fabrication of multifunctional nanosystems, known as nanomachines. Such devices may, as an example, sense the presence of disease, deliver a drug to the site of disease, and release the drug at that site.

We thank Drs. Darren Brown, Fernando Ferrer, Edward Monosov, Lea Rudee, and Michael Sailor for their help with this work. Oriaku A. Kas-Osoka assisted with qdot synthesis, and Robbin Newlin assisted with histology. This study was supported by grants from the National Cancer Institute (CA82713), the Department of Defense (DAMD 17-02-1-0315), and the Komen Foundation (99–3339) (to E.R.), and the David and Lucile Packard Foundation and the Defense Advanced Research Projects Agency (to S.N.B.). M.E.A. received support from the American-Scandinavian Foundation; W.C.W.C., received support from the National Institutes of Health; and P.L., received support from the Academy of Finland and the Finnish Cultural Foundation.

1. Niemeyer, C. M. (2001) *Angew. Chem.* **40,** 4128–4158.
2. Chan, W. C., Maxwell, D. J., Gao, X., Bailey, R. E., Han, M. & Nie, S. (2002) *Curr. Opin. Biotechnol.* **13,** 40–46.
3. Alivisatos, A. P. (1996) *Science* **271,** 933–937.
4. Han, M., Gao, X., Su, J. Z. & Nie, S. (2001) *Nat. Biotechnol.* **19,** 631–635.
5. Ruoslahti, E. (2000) *Semin. Cancer Biol.* **10,** 435–442.
6. Arap, W., Pasqualini, R. & Ruoslahti, E. (1998) *Science* **279,** 377–380.
7. Pasqualini, R., Koivunen, E. & Ruoslahti, E. (1997) *Nat. Biotechnol.* **15,** 542–546.
8. Pasqualini, R. & Ruoslahti, E. (1996) *Nature (London)* **380,** 364–366.
9. Rajotte, D. & Ruoslahti, E. (1999) *J. Biol. Chem.* **274,** 11593–11598.
10. Porkka, K., Laakkonen, P., Hoffman, J. A., Bernasconi, M. & Ruoslahti, E. (2002) *Proc. Natl. Acad. Sci. USA* **99,** 7444–7449.
11. Laakkonen, P., Porkka, K., Hoffman, J. A. & Ruoslahti, E. (2002) *Nat. Med.* **8,** 751–755.

12. Peng, X., Schlamp, M. C., Kadavanich, A. V. & Alivisatos, A. P. (1997) *J. Am. Chem. Soc.* **119,** 7019–7029.
13. Murray, C. B., Norris, D. J. & Bawendi, M. G. (1993) *J. Am. Chem. Soc.* **115,** 8706–8715.
14. Dabbousi, B. O., Rodriguez-Viejo, J., Mikulec, F. V., Heine, J. R., Mattoussi, H., Ober, R., Jensen, K. F. & Bawendi, M. G. (1997) *J. Phys. Chem. B* **101,** 9463–9475.
15. Hines, M. A. & Guyot-Sionnest, P. (1996) *J. Phys. Chem. B* **100,** 468–471.
16. Chan, W. C. & Nie, S. (1998) *Science* **281,** 2016–2018.
17. Mitchell, G. P., Mirkin, C. A. & Letsinger, R. L. (1999) *J. Am. Chem. Soc.* **121,** 8122–8123.
18. Rajotte, D., Arap, W., Hagedorn, M., Koivunen, E., Pasqualini, R. & Ruoslahti, E. (1998) *J. Clin. Invest.* **102,** 430–437.
19. Liu, V. A., Jastromb, W. E. & Bhatia, S. N. (2002) *J. Biomed. Mater. Res.* **60,** 126–134.
20. Kahan, F. M., Kropp, H., Sundelof, J. G. & Birnbaum, J. (1983) *J. Antimicrob. Chemother.* **12,** Suppl. D, 1–35.
21. Breiteneder-Geleff, S., Soleiman, A., Kowalski, H., Horvat, R., Amann, G., Kriehuber, E., Diem, K., Weninger, W., Tschachler, E., Alitalo, K., *et al.* (1999) *Am. J. Pathol.* **154,** 385–394.
22. Gref, R., Minamitake, Y., Peracchia, M. T., Trubetskoy, V., Torchilin, V. & Langer, R. (1994) *Science* **263,** 1600–1603.
23. Nie, S. & Emory, S. R. (1997) *Science* **275,** 1102–1106.
24. Bruchez, M., Jr., Moronne, M., Gin, P., Weiss, S. & Alivisatos, A. P. (1998) *Science* **281,** 2013–2016.
25. Schreder, B., Schmidt, T., Ptatschek, V., Winkler, U., Materny, A., Umbach, E., Lerch, M., Muller, G., Kiefer, W. & Spanhel, L. (2000) *J. Phys. Chem. B* **104,** 1677–1685.
26. Micic, O. I., Cheong, H. M., Fu, H., Zunger, A., Sprague, J. R., Mascarenhas, A. & Nozik, A. J. (1997) *J. Phys. Chem. B* **101,** 4904–4912.
27. Lewin, M., Carlesso, N., Tung, C., Tang, X., Cory, D., Scadden, D. T. & Weissleder, R. (2000) *Nat. Biotechnol.* **18,** 410–414.
28. Bulte, J. W. M., Douglas, T., Witwer, B., Zhang, S., Strable, E., Lewis, B. K., Zywicke, H., Miller, B., van Gelderen, P., Moskowitz, B. M., *et al.* (2001) *Nat. Biotechnol.* **19,** 1141–1147.
29. Kroto, H. W., Heath, J. R., O'Brien, S. C., Curl, R. F. & Smalley, R. E. (1985) *Nature (London)* **318,** 162–163.
30. Heath, J. R. (1998) *Nature (London)* **393,** 730–731.
31. Frechet, J. M. (1994) *Science* **263,** 1710–1715.
32. Grayson, S. M. (2001) *Chem. Rev.* **101,** 3819–3868.
33. Hood, J. D., Bednarski, M., Frausto, R., Guccione, S., Reisfeld, R. A., Xiang, R. & Cheresh, D. A. (2002) *Science* **296,** 2404–2407.